

similar to those published by Duggan et al. (9). Therefore, our results from the cutaneous and oral administration are essentially in agreement with the metabolic pattern reported by others for intravenous, oral and rectal routes, which suggests that the metabolism of indomethacin is independent of the route of administration.

References

- (1) Price, N. M., Schmitt, L. G., McGuire, J., Shaw, J. E., Trobough, G. (1981) *Clin. Pharmacol. Ther.* 414-419.
- (2) Armstrong, P. W., Armstrong, J. A., Marks, G. S. (1980) *Am. J. Cardiology* 670-676.
- (3) Arndts, D., Arndts, K. (1984) *Eur. J. Clin. Pharmacol.* 26, 79-85.
- (4) Inagi, T., Muramatsu, T., Nagai, H. (1979) *Yakuri to Chiryō* 7, Suppl. 1, 35.
- (5) Bayne, W. F., East, T., Dye, D. (1981) *J. Pharm. Sci.* 70, 458-459.
- (6) Bernstein, M. S., Evans, M. A. (1982) *J. Chromatogr.* 229, 179-187.
- (7) Evans, M. A. (1980) *J. Pharm. Sci.* 69, 219-220.
- (8) Kwan, K. C., Breault, G. O., Umbenhauer, E. R., McMahon, F. G., Duggan, D. E. (1976) *J. Pharmacokin. Biopharm.* 4, 255-280.
- (9) Duggan, D. E., Hogans, A. F., Kwan, K. C., McMahon, F. G. (1972) *Exp. Ther.* 181, 563-575.

Kinetic Analysis of Transdermal Nitroglycerin Delivery

Richard H. Guy^{1,3} and Jonathan Hadgraft²

Received: January 8, 1985; Accepted: March 25, 1985.

Abstract: The current success of transdermal nitroglycerin delivery systems has focussed much attention upon the skin as a portal of drug entry into the systemic circulation. Although there are multiple potential problems associated with this administration route to elicit central effects, considerable efforts are being made to identify transdermal drug delivery candidates and to determine whether a sufficient percutaneous input rate can be achieved such that therapeutic levels in the biophase may be maintained. The purpose of this work is to develop a physically-based kinetic model of percutaneous absorption, which includes delivery system input. Both zero-order and first-order situations are considered and the model is employed to analyze nitroglycerin plasma concentration vs. time data following transdermal delivery both from a controlled-release patch and from an ointment. The kinetic model includes rate parameters which relate to drug transport across the stratum corneum, to further diffusion across the viable epidermis and to the competition for substrate between these two layers of skin tissue. We show how these kinetic constants may be determined physicochemically and used, in conjunction with designated (delivery system) input rates and established systemic elimination kinetics, to predict plasma concentrations as a function of time. The agreement with human *in vivo* data for nitroglycerin, delivered from either a patch or a more conventional vehicle, is good and suggests that the simulation proposed may enable facile estimation of the feasibility of transdermal drug delivery.

The delivery of drugs via the skin to elicit systemic effects is attractive for many reasons (1-3). For example, hepatic first-pass metabolism may be circumvented, a steady, sustained plasma concentration of drug may be maintained, dosing frequency and dose magnitude may be reduced and, consequently, fewer side-effects and better patient compliance may

be expected. Furthermore, a properly designed delivery device should lead to lower inter- and intra-patient variation, and a topical system has the unique advantage of permitting rapid termination of therapy in problematic situations. Of course, transdermal delivery also has limitations: the drug must be pharmacologically potent (normal daily dose requirements of a few milligrams or less) because the skin is a very good barrier to chemical ingress; thus the compound must be absorbable to some extent and its chemical properties should include, therefore, (1) a moderate molecular weight (in the order of 1000 daltons or less) and (2) reasonable oil and water solubility (*ca.* 1 mg/ml).

Transdermal delivery of nitroglycerin (GTN) is presently the most successful example of this mode of drug administration (4-6). In the U.S., three GTN devices are commercially available and are in competition with sublingual and ointment formulations of the vasodilating drug. The relatively recent acquisition of GTN pharmacokinetic data has allowed favorable conclusions pertaining to the efficacy of transdermal delivery to be drawn. Of the three marketed devices, two are of the matrix variety, the other is multi-laminate and includes a "rate-controlling" membrane. The degree of rate-control afforded by this membrane has been comprehensively defined in a recent paper by Good (4).

The purpose of the work described here is to present a novel analysis of GTN pharmacokinetics following transdermal delivery. The approach employs a physically based kinetic model of percutaneous absorption, the details and certain applications of which have been reported elsewhere (7-9). We make use of the *in vitro* and *in vivo* release characteristics, which have been described for the membrane-modulated GTN device (4, 10), and, where possible, compare the derived behavior to that expected and shown by the conventional ointment preparation. We show that the proposed kinetic model is able to simulate very adequately the observed *in vivo* disposition of GTN. The model accomplishes this correlation

¹ Departments of Pharmacy and Pharmaceutical Chemistry, School of Pharmacy, University of California, San Francisco, San Francisco, CA 94143, USA

² Department of Pharmacy, University of Nottingham, University Park, Nottingham, NG72RD, United Kingdom

³ Correspondence

by estimating *transdermal* kinetic parameters from physicochemical principles alone. It follows, therefore, that the theoretical rationale may be used predictively to identify candidates for transdermal delivery and to establish optimum release characteristics for the system employed.

The Model

The pharmacokinetic model is shown schematically in Figure 1. The representation involves extension of the simulation proposed by Guy et al. (7) to include zero-order (k^0) or first-order (k^1) release to the skin surface from the applied formulation (e. g., patch or ointment). Furthermore, in the discussions presented here, we shall use the approach to determine plasma levels of penetrant rather than urinary excretion rates [the focus of most of the earlier applications of the model (7, 8)].

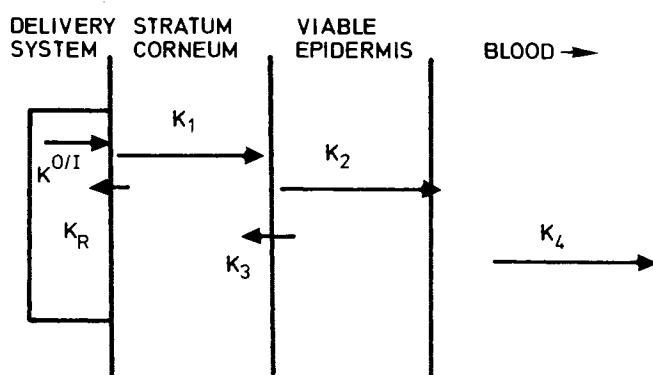


Fig. 1 Schematic representation of the pharmacokinetic model.

The rate parameters identified in the model have the following significance:

1. k^0 (amount per unit area per unit time) and k^1 (time^{-1}) describe, respectively, zero-order and first-order drug release from the applied topical formulation. In the case of the membrane-modulated devices for scopolamine and nitroglycerin (11, 4), both zero-order and first-order release behavior is observed. The former originates from the expected membrane-controlled leaching of drug out of the reservoir. The latter results from the fact that the adhesive retaining the patch on the skin surface contains a loading dose of the drug which facilitates the more rapid attainment of desired plasma levels. Release experiments have shown that the loading dose is delivered into the skin according to first-order kinetics (11). In the case of an ointment, we shall assume, in this paper, that release can be adequately modelled by a k^1 process; for nitroglycerin, it will be shown, this is a reasonable approximation.

2. k_r appears in the model for completeness but may be expected, in most instances, to have a very low value. The parameter allows for competition for the drug between the applied formulation (e. g., ointment or patch adhesive) and the stratum corneum. If the delivery system is formulated appropriately, then one would expect partitioning into the skin to be favored and k_r to be small. On the other hand, for compounds which show very low affinity for the skin, then a high k_r value can be used to describe the slow interfacial passage of material at the delivery system-skin boundary.

3. k_1 and k_2 are first-order rate constants that describe drug diffusion through the stratum corneum and viable epidermal

tissue, respectively. The kinetic parameters may be equated with the ratio of the corresponding diffusion coefficient (D) to the diffusion path length (h) squared in the two tissue layers (7), i. e.,

$$k_1 = D_{sc}/h_{sc}^2 ; \quad k_2 = D_{vt}/h_{vt}^2 \quad (1)$$

If we assume ideal behavior for the stratum corneum and viable tissue, then h_{sc} and h_{vt} should be constant for all penetrants, and k_1 and k_2 [from the Stokes-Einstein relationship (12)] may then be shown to be simple functions of drug molecular weight (M):

$$k_1 = C_1 M^{-1/3} \quad (2)$$

$$k_2 = C_2 M^{-1/3} \quad (3)$$

where C_1 and C_2 are constants. k_1 and k_2 values for benzoic acid (k_1^{BA} and k_2^{BA}) have been established by earlier work (2), and hence we may use eqns 2 and 3 to find k_1 and k_2 for nitroglycerin (k_1^{GTN} and k_2^{GTN}) by simple ratio:

$$k_1^{GTN} = k_1^{BA} (M^{BA}/M^{GTN})^{1/3} \quad (4)$$

$$k_2^{GTN} = k_2^{BA} (M^{BA}/M^{GTN})^{1/3} \quad (5)$$

4. The model depicted in Figure 1 assumes the skin to be biphasic and divided into essentially lipophilic stratum corneum and aqueous viable tissue. The discussion above relating to k_1 and k_2 further assumes that transport through these two tissue layers is somewhat ideal and dependent only upon molecular size. This latter assumption is too severe because it does not take into account the differential affinities that different penetrants will show towards stratum corneum and viable tissue. The k_3 rate constant is used, therefore, to compensate for this insensitivity and has been chosen in such a way that the model may be used predictively. k_3 allows for specific interactions [e. g., binding or reservoir effects (13)] between the penetrant and the stratum corneum. The larger k_3 , the greater the affinity of the absorbing drug for the stratum corneum, and vice versa. It follows that the ratio k_3/k_2 then provides an "effective partition coefficient" of the drug between stratum corneum and viable tissue, and this identity permits a predictive entry point. We have shown in previous work (14, 15) that, for a broad selection of topically delivered chemicals *in vivo* in man, k_3/k_2 is linearly related to the simple octanol-water partition coefficient (K):

$$k_3/k_2 \approx K/5 \quad (6)$$

It is now possible to estimate the kinetic parameters of the model describing transdermal movement purely on the basis of the drug's physicochemical properties. Expressions like eqns (4) and (5) allow k_1 and k_2 to be found; then eqn (6) (i. e., the value of K) in conjunction with k_2 permits evaluation of k_3 . The rationale of this stage of the argument describing the model's development is important and is worth reiteration: We first use an ideal transport relationship to characterize drug diffusion through stratum corneum and viable tissue. The insensitivity of this approach is then compensated for by k_3 which is, in turn, closely related to a basic oil-water partition coefficient. Prediction of k_1 , k_2 and k_3 is thus possible. *A priori* prediction of "true" transport parameters across the skin remains a future goal. The present simulation, we believe, recognizes the problems involved in attaining such an objective and offers an alternative, not necessarily perfect, but pragmatic approach.

5. Finally, k_4 describes drug elimination from the blood. The concentration of drug in the cutaneous capillaries is assumed to be the same as that in the systemic circulation. Of course, the elimination process may be more complex than a single-exponential decay in which case a more complicated function should replace k_4 (16). This parameter cannot be predicted physicochemically and must be determined, for example, by measuring as a function of time, the decay of drug concentration in plasma following intravenous administration.

Mathematically, the model depicted in Figure 1 may be represented by a series of differential equations:

(A) for zero-order input (from a delivery system of thickness l):

$$dc_0/dt = -k^0/l + V_1 k_r c_1 / V_0 \quad (7)$$

$$dc_1/dt = V_0 k^0 / V_1 l - (k_r + k_1) c_1 \quad (8)$$

$$dc_2/dt = V_1 k_1 c_1 / V_2 - k_2 c_2 + V_3 k_3 c_3 / V_2 \quad (9)$$

$$dc_3/dt = V_2 k_2 c_2 / V_3 - (k_3 + k_4) c_3 \quad (10)$$

(B) for first-order input:

$$dc_0/dt = -k^1 c_0 + V_1 k_r c_1 / V_0 \quad (11)$$

$$dc_1/dt = V_0 k^1 / V_1 - (k_r + k_1) c_1 \quad (12)$$

and the corresponding equations for dc_2/dt and dc_3/dt are, of course, given by eqns (9) and (10). In these expressions (eqns 6–12), V_i and c_i are, respectively, the volume of and the drug concentration in compartment i .

The equations for the two cases are easily solved (17) to give expressions for the plasma concentration (c_3). The results are: – for *zero-order* input:

$$c_3 = \frac{A k^0 k_1 k_2}{V_3} \left\{ \frac{1}{\alpha \beta \epsilon} - \frac{\exp(-\alpha t)}{[\alpha(\alpha - \beta)(\alpha - \epsilon)]} - \frac{\exp(-\beta t)}{[\beta(\beta - \alpha)(\beta - \epsilon)]} - \frac{\exp(-\epsilon t)}{[\epsilon(\epsilon - \alpha)(\epsilon - \beta)]} \right\} \quad (13)$$

for *first-order* input:

$$c_3 = \frac{M_\infty k^1 k_1 k_2}{V_3} \left\{ \frac{\exp(-\alpha t)}{[(\beta - \alpha)(\alpha - \omega)(\alpha - \mu)]} + \frac{\exp(-\beta t)}{[(\alpha - \beta)(\beta - \omega)(\beta - \mu)]} + \frac{\exp(-\omega t)}{[(\alpha - \omega)(\omega - \beta)(\omega - \mu)]} + \frac{\exp(-\mu t)}{[(\alpha - \mu)(\mu - \beta)(\mu - \omega)]} \right\} \quad (14)$$

In eqn (13), A is the surface area of the delivery system and $\epsilon = (k_r + k_1)$; in eqn (14) M_∞ is the total amount of drug applied (i. e., $M_\infty = A l c_0 =$ drug concentration in vehicle \times area of application \times thickness of applied phase). α and β and ω and μ are the roots of quadratics and are defined by the following pairs of equations:

$$(\alpha + \beta) = k_2 + k_3 + k_4 ; \quad \alpha \beta = k_2 k_4 \quad (15)$$

$$(\omega + \mu) = k^1 + k_r + k_1 ; \quad \omega \mu = k^1 k_1 \quad (16)$$

Thus, if one is able to (a) characterize the delivery system, (b) estimate reliably the transdermal rate parameters, and (c) obtain systemic elimination kinetics (k_4) and volume of distribution (V_3) information, then c_3 may be predicted. Alternatively, one may choose a target c_3 value to determine the necessary input rate characteristics for a candidate transdermal drug delivery system. Below, we demonstrate that the former approach may be successfully applied to nitroglycerin administered via the skin. Hence, we also show, by implica-

tion, that the latter strategy may prove to be an effective means of assessing the feasibility of delivering a chemical systemically using the skin as the route of entry.

Results and Discussion

The parameters necessary to calculate c_3 using eqns (13) and (14) have been obtained in the following way:

(a) k_1 and k_2 are calculated with eqns (4) and (5) respectively, using values of $k_1^{BA} = 0.18 \text{ h}^{-1}$ and $k_2^{BA} = 2.90 \text{ h}^{-1}$ (2) and the appropriate molecular weights ($M^{BA} = 122$, $M^{GTN} = 227$). Hence, we find that $k_1^{GTN} = 0.15 \text{ h}^{-1}$ and $k_2^{GTN} = 2.36 \text{ h}^{-1}$.

(b) The ratio k_3/k_2 is determined from the published (18) octanol-water partition coefficient ($K = 112$) and eqn (6). Then, with the value of k_2 found above, it follows that $k_3 = 53 \text{ h}^{-1}$.

(c) Nitroglycerin is very rapidly cleared from the circulation and its plasma half-life is $2.3 \pm 0.6 \text{ min}$ (19). In the calculations below, therefore, elimination half-lives for the drug of 1.7, 2.3, and 2.9 min have been chosen, i. e., we determine c_3 using one of three k_4 values: 24.75 h^{-1} , 18.24 h^{-1} , and 14.44 h^{-1} , which correspond to the range of biological variability encountered in man (mean – s. d., mean, and mean + s. d.).

(d) V_3 is the volume of distribution for GTN, reported to be $3.3 \pm 1.2 \text{ l/kg}$ (19) or 231 ± 84 liters for a 70 kg adult. Again calculations have been made to indicate the effect of variability in V_3 on the predicted plasma concentration-time profile.

(e) The remaining parameters are k^0 , k^1 and k_r . We assume that the affinity of GTN for the skin is much greater than its preference for the delivery system and that k_r is therefore small. We have chosen $k_r = 1 \times 10^{-6} \text{ h}^{-1}$. The release rate of GTN from the membrane-controlled delivery system, which is presently on the market, has been measured (4): $k^0 = 0.036 \text{ mg/cm}^2/\text{h}$. We have based our calculations upon the application of a 10 cm^2 patch containing a total of 25 mg GTN, 23 mg of which are initially localized in the reservoir, 2 mg in the adhesive (4). To simulate GTN release from the patch, both eqns (13) and (14) are required (4, 11). The former with the above k^0 and $A = 10 \text{ cm}^2$ describes the membrane-controlled leaching of drug from the reservoir. The latter represents input of GTN due to the “loading” dose in the adhesive. For scopolamine delivery from a transdermal system, release from the adhesive has been shown to be first-order with $k^1 = 1.3 \text{ h}^{-1}$ (11). Since the design of the GTN patch is similar, we have assumed an equivalent k^1 in our calculations.

We can now calculate c_3 for GTN following transdermal delivery from a membrane-controlled patch. Figure 2 compares the prediction, which is obtained when mean values for V_3 and k_4 (231 liters and 18.24 h^{-1} , respectively) are used, with the average (\pm S. E.) *in vivo* data reported by Good (4). The prediction is presented in three parts: that is, zero-order [eqn (13)] and first-order [eqn (14)] contributions being shown together with the resulting summation. It can be seen that the predicted profile is in very reasonable agreement with the human results and that the discrepancies between model and experiment are within the variability that may be expected in a typical subject population. Figure 2 also shows the crucial role of the loading dose in the adhesive for controlled transdermal GTN therapy. Establishment of the target, constant plasma concentration, is significantly enhanced by the “priming” source of drug in the contact layer of the patch.

The accuracy of our predictions can also be explored by studying the “theoretical” range of possible plasma concentra-

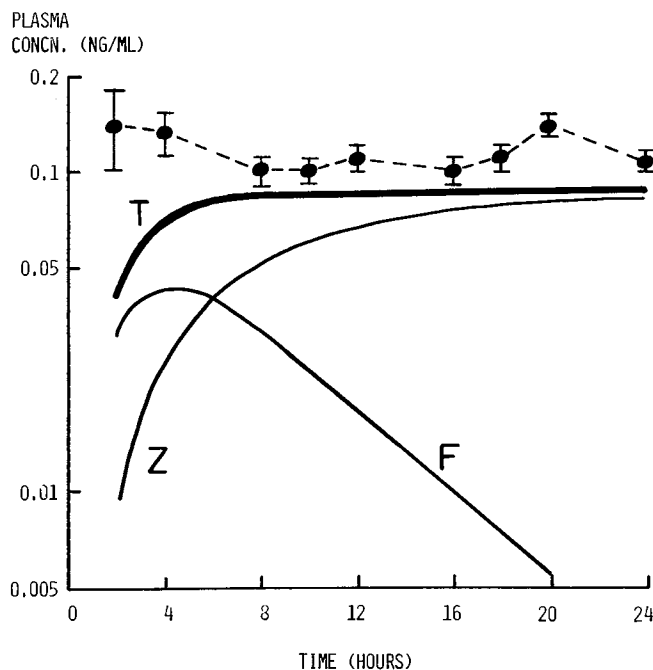


Fig. 2 Prediction of GTN plasma concentration following transdermal delivery from a "membrane-controlled" patch. Curve F represents first-order input of drug from the 'priming' dose in the contact adhesive [according to eqn (14)]. Curve Z indicates membrane-controlled leaching from the reservoir [according to eqn (13)]. The summation is shown by curve T. The rate constants employed are: $k^0 = 0.036 \text{ mg/cm}^2/\text{h}$, $k^1 = 1.3 \text{ h}^{-1}$, $k_r = 1 \times 10^{-6} \text{ h}^{-1}$, $k_1 = 0.15 \text{ h}^{-1}$, $k_2 = 2.36 \text{ h}^{-1}$, $k_3 = 53 \text{ h}^{-1}$, $k_4 = 18.24 \text{ h}^{-1}$, $V_3 = 231 \text{ liters}$. The origin of the parameters is discussed in the text. The solid circles (\pm S. E.) are published *in vivo* data (4) ($N=12$).

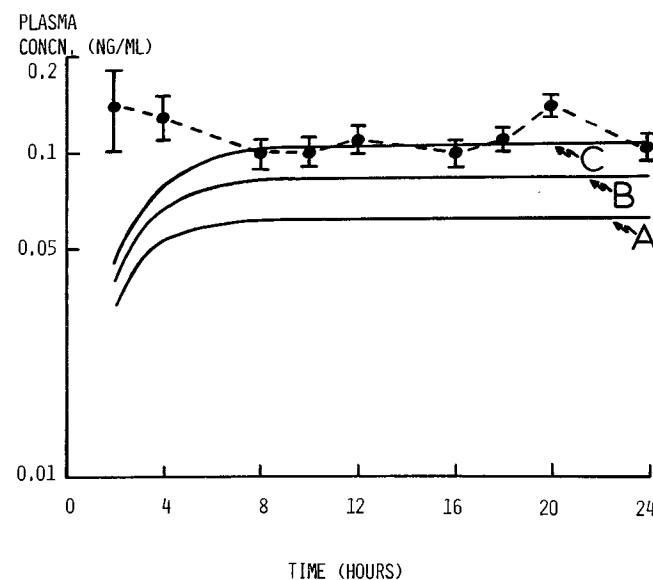


Fig. 3 Prediction of GTN plasma concentration following transdermal delivery from a "membrane-controlled" patch. k^0 , k^1 , k_r , k_1 - k_3 and V_3 are as given in the legend to Figure 2. Curve A uses $k_4 = 24.77 \text{ h}^{-1}$ [mean (19) + s. d.], curve B has $k_4 = 18.24 \text{ h}^{-1}$ [mean (19)] and curve C employs $k_4 = 14.44 \text{ h}^{-1}$ [mean (19) - s. d.]. The solid circles (\pm S. E.) are published *in vivo* data (4) ($N=12$).

tions using the biological variability indicated by the *in vivo* volume of distribution and elimination half-life values (see above). In Figure 3, we fix V_3 at the mean value of 231 liters

and allow k_4 to vary from one standard deviation below to one standard deviation above the mean. Figure 4 shows the opposite experiment, in which the elimination half-life is held constant at its average value (2.3 minutes) and three V_3 values are considered (mean - s. d., mean, mean + s. d.). For comparison, we again show the mean *in vivo* plasma concentrations together with their respective standard errors (4). It is clear, that for GTN, because of the pharmacokinetic variability encountered, further refinement to our model predictions cannot be justified at the present time.

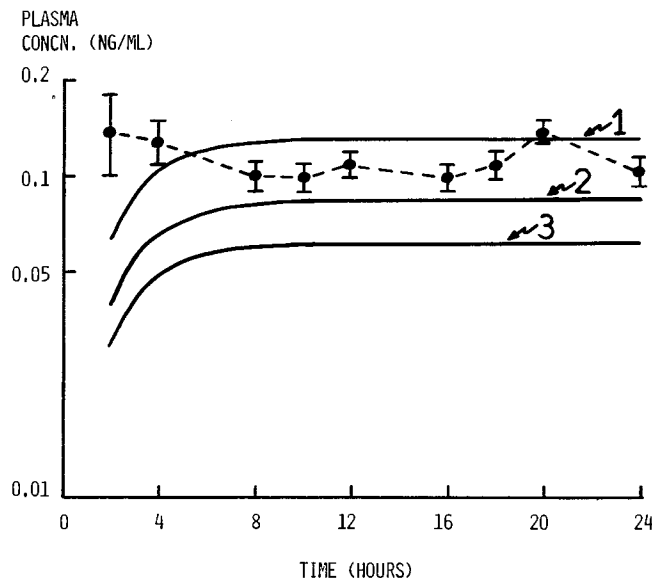


Fig. 4 Prediction of GTN plasma concentration following transdermal delivery from a "membrane-controlled" patch. k^0 , k^1 , k_r , k_1 - k_4 are as given in the legend to Figure 2. Curve 1 uses $V_3 = 147 \text{ liters}$ [mean (19) - s. d.], curve 2 has $V_3 = 231 \text{ liters}$ [mean (19)], and curve 3 employs $V_3 = 315 \text{ liters}$ [mean (19) + s. d.]. The solid circles (\pm S. E.) are published *in vivo* data (4) ($N=12$).

The ability to mirror successfully the plasma concentration-time course is encouraging. It should be pointed out, of course, that the zero-order input rate required to achieve a desired steady-state plasma concentration (c_3^{SS}) can be found from the simple "rate in = rate out" equality [eqn (17)]

$$Ak^0 = V_3 k_4 c_3^{SS} \quad (17)$$

Hence, with k^0 set at $36 \mu\text{g/cm}^2/\text{h}$, $A=10 \text{ cm}^2$ and V_3 and k_4 taking their average values (19), we find $c_3^{SS} = 0.086 \text{ ng/ml}$, which is exactly the limiting c_3 in Figure 2. In this paper, we report the additional steps by which the approach (i. e., the kinetics of the approach) to steady-state can be calculated and modified by engineering details within the patch (e. g., adhesive type, release characteristics and loading dose). The time-course of the approach to steady-state and questions relating to the location of the rate-determining step (and hence the feasibility of the transdermal mode of administration) are now accessible through the pharmacokinetic model described.

The results for the controlled delivery system may be contrasted with the behavior typical of a more conventional topical formulation, an ointment. In this case, we assume exclusively first-order delivery kinetics and determine the plasma concentration with eqn (14) alone. The calculations are based upon application of 0.25 ml of 2% ointment [about $\frac{1}{2}$ inch of the commercial preparation (22)] to a skin surface area of 10 cm^2 . To illustrate the kinetic profile, we use k_1 - k_3 values

as before and choose the mean elimination half-life (19) of 2.3 minutes to obtain k_4 . k_r is again set to be very small: $1 \times 10^{-6} \text{ h}^{-1}$. In Figure 5, we then plot c_3 as a function of time following a single administration of the ointment for three different values of k^I : 6.5 h^{-1} , 1.3 h^{-1} , 0.26 h^{-1} . The medium value is that which was assigned to describe release from the adhesive layer of the patch (see above). The high and low values are, respectively, five times and one-fifth of 1.3 h^{-1} . The k^I values correspond to input half-lives of between 0.1 and 2.7 h. Finally, in Figure 6, for $k^I = 1.3 \text{ h}^{-1}$, the plasma level as a function of time following three 8-hourly topical doses is calculated and compared with mean ($\pm \text{SE}$) human *in vivo* data (4).

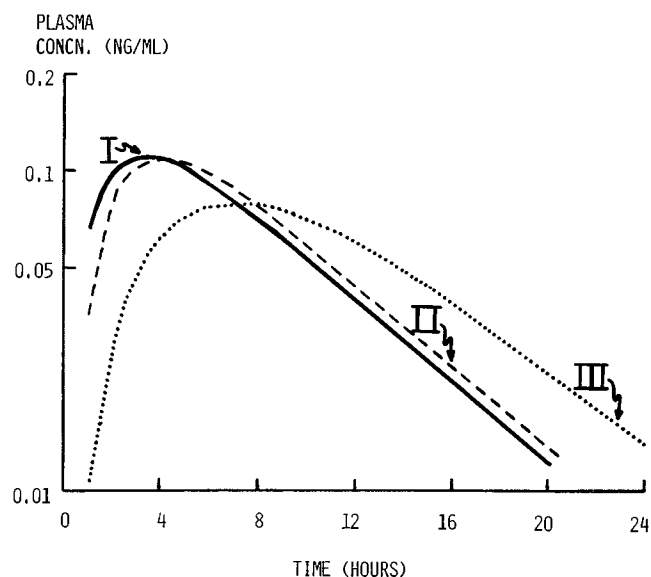


Fig. 5 Simulated GTN plasma concentration following a single topical administration of a 2% ointment. The calculations assume a vehicle volume of 0.25 ml applied over an area of 10 cm^2 . Curves are shown for three first-order release rates from the ointment: $k^I = 6.5 \text{ h}^{-1}$ (Curve I), $k^I = 1.3 \text{ h}^{-1}$ (Curve II), $k^I = 0.26 \text{ h}^{-1}$ (Curve III). The other rate constants employed are: $k_r = 1 \times 10^{-6} \text{ h}^{-1}$, $k_1 = 0.15 \text{ h}^{-1}$, $k_2 = 2.36 \text{ h}^{-1}$, $k_3 = 53 \text{ h}^{-1}$ and $k_4 = 18.24 \text{ h}^{-1}$.

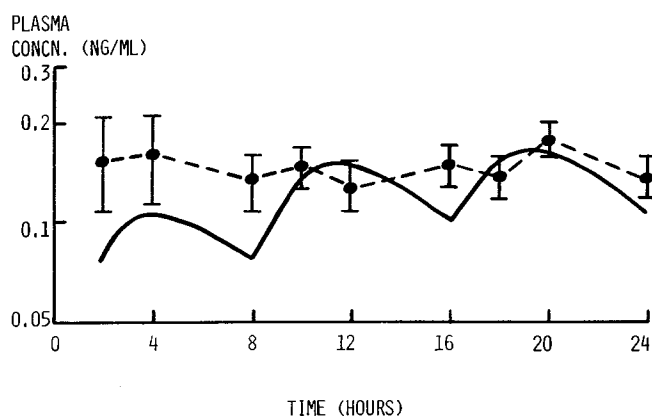


Fig. 6 Simulated GTN plasma concentration following 8-hourly multiple administration of a 2% ointment. Each dose is 0.25 ml applied over an area of 10 cm^2 . The rate constants employed are: $k^I = 1.3 \text{ h}^{-1}$, $k_r = 1 \times 10^{-6} \text{ h}^{-1}$, $k_1 = 0.15 \text{ h}^{-1}$, $k_2 = 2.36 \text{ h}^{-1}$, $k_3 = 53 \text{ h}^{-1}$, $k_4 = 18.24 \text{ h}^{-1}$. The solid circles ($\pm \text{S.E.}$) are published *in vivo* data (4) ($N=12$).

Figure 5 shows that the two faster k^I values, although differing by a factor of 5, give essentially the same kinetic profiles. The smallest k^I (0.26 h^{-1}) leads to a different profile because its value is approaching that of k_1 (i.e., 0.15 h^{-1}); hence absorption rate control is no longer determined exclusively by diffusion of GTN across the stratum corneum. The multiple-dose profile in Figure 6 demonstrates that GTN ointment administration every 8 h leads to a rapid establishment of steady-state kinetics. Once again, the agreement between simulation and experiment is good and the differences fall within observed biological variability.

In conclusion, it can be stated that the kinetic model proposed in this paper very adequately predicts the plasma concentration-time relationships of GTN following transdermal delivery. The approach makes use of the *in vitro* release characteristics of the applied delivery system and of known GTN elimination kinetics and volume of distribution. The simulation assesses *transdermal* kinetic processes on the basis of the drug's physical chemistry alone. The viability of the approach is implied by its success in modelling available *in vivo* data. Other work (17, 23) suggests that equally impressive agreement between theoretical prediction and *in vivo* reality can be achieved for two other transdermally delivered agents, scopolamine and clonidine. It seems possible, therefore, that this predictive pathway may facilitate (1) the assessment of candidate drugs being considered for transcutaneous delivery, and (2) the determination of the necessary input kinetics required to achieve therapeutic drug levels in the biophase.

Acknowledgements

We thank NIOSH (OH-01830), Ciba-Geigy and Vick International for financial support and Andrea Mazel for manuscript preparation. RHG is the recipient of a Special Emphasis Research Career Award (1-K01-00017-01) from the National Institute of Occupational Safety and Health. A preliminary account of this work was presented at the 11th International Symposium on Controlled Release of Bioactive Materials, Fort Lauderdale, Florida, 1984.

References

- (1) Chien, Y. W. (1982) *Novel Drug Delivery Systems*, pp. 149–217, Marcel Dekker Inc., New York.
- (2) Chandrasekaran, S. K., Shaw, J. E. (1980) *Controlled Release of Bioactive Materials* (Baker, R., ed.), pp. 99–106, Academic Press, New York.
- (3) Chandrasekaran, S. K., Benson, H., Urquhart, J. (1978) *Sustained and Controlled Release Drug Delivery Systems* (Robinson, J. R., ed.) pp. 557–593, Marcel Dekker, Inc., New York.
- (4) Good, W. R. (1983) *Drug Dev. Ind. Pharm.* 9, 647–670.
- (5) Karim, A. (1983) *Drug Dev. Ind. Pharm.* 9, 671–689.
- (6) Keith, A. D. (1983) *Drug Dev. Ind. Pharm.* 9, 605–625.
- (7) Guy, R. H., Hadgraft, J., Maibach, H. I. (1982) *Internat. J. Pharmaceut.* 11, 119–129.
- (8) Guy, R. H., Hadgraft, J., Maibach, H. I. (1983) *Internat. J. Pharmaceut.* 17, 23–28.
- (9) Guy, R. H., Hadgraft, J. (1984) *J. Pharm. Sci.* 73, 883–888.
- (10) Heilman, K. (1984) *Therapeutic Systems*, 2nd edition, pp. 37–48, Thieme-Stratton, Inc., Stuttgart (and references therein).
- (11) Chandrasekaran, S. K., Bayne, W., Shaw, J. E. (1978) *J. Pharm. Sci.* 67, 1370–1374.
- (12) Atkins, P. W. (1978) *Physical Chemistry*, pp. 833–843, Oxford University Press, Oxford.
- (13) Wester, R. C., Maibach, H. I. (1983) *Drug Metab. Rev.* 14, 169–205.

- (14) Guy, R. H., Hadgraft, J., Maibach, H. I. (1985) *Toxicol. Appl. Pharmacol.* 78, 123–129.
- (15) Guy, R. H., Hadgraft, J., Maibach, H. I. (1985) *Dermal Exposure Related to Pesticide Use* (Honeycutt, R. C., Zweig, G., Ragsdale, N. N., eds.) pp. 19–31, American Chemical Society, Washington, D.C.
- (16) Rowland, M., Tozer, T. N. (1980) *Clinical Pharmacokinetics: Concepts and Applications*, pp. 79–94, Lea & Febiger, Philadelphia.
- (17) Guy, R. H., Hadgraft, J. (1985) *J. Control. Res.* 1, 177–182.
- (18) Leo, A., Hansch, C., Elkins, D. (1971) *Chem. Rev.* 71, 525–616.
- (19) Gilman, A. G., Goodman, L. S., Gilman, A. (1985) *The Pharmacological Basis of Therapeutics* (7th edition), Macmillan, New York, in press; McNiff, E. F., Yacobi, A., Young-Chang, F. M., Golden, L. H., Goldfarb, A., Fung, H.-L. (1981) *J. Pharm. Sci.* 70, 1054–1058.
- (20) Wester, R. C., Noonan, P. K., Smeach, S., Kosobud, L. (1983) *J. Pharm. Sci.* 72, 745–748.
- (21) Müller, P., Imhof, P. R., Burkart, F., Chu, L.-C., Gérardin, A. (1982) *Eur. J. Clin. Pharmacol.* 22, 473–480.
- (22) NITRO-BID® ointment (2% nitroglycerin), Marion Laboratories Inc., Kansas City, MO.
- (23) Guy, R. H., Hadgraft, J. (1985) *J. Pharm. Sci.*, in press.

Computer Modeling of the Pharmacokinetics of Fluorouracil and Thymine and Their Kinetic Interaction in Normal Dogs⁵

Joseph M. Covey^{1,2,3,4} and James A. Straw¹

Received: January 2, 1985; accepted: March 21, 1985.

Abstract: The kinetic behavior of thymine and 5-fluorouracil has been shown to be non-linear and mediated largely by saturable metabolic processes. *In vivo* estimates of the Michaelis-Menten parameters V_{max} and K_m were obtained from constant infusion data in normal dogs using a system of balance equations that equate drug input with total output at steady-state. These estimates were then successfully used to simulate both steady-state and post-infusion plasma concentration-time curves for both compounds over a range of saturating and non-saturating conditions. It has been shown previously that estimates of V_{max} and K_m obtained from dynamic data can be incorrect if an inappropriate compartmental model is used in the analysis. Determining the Michaelis-Menten parameters at steady-state eliminates this difficulty. Moreover, the use of steady-state derived values to simulate post-infusion data confirms the validity of this technique. The kinetic interaction between thymine and 5-fluorouracil was investigated as a case of competitive metabolic inhibition *in vivo* by calculating K_i values from data obtained during simultaneous constant infusions of the two compounds. These values were then used in conjunction with a series of differential equations incorporating reciprocal metabolic effects to simulate the effect of thymine on FU plasma concentration.

We have shown previously that the elimination of the pyrimidines thymine (Thy), thymidine (dThd), and

fluorouracil (FUra) in normal dogs is mediated in part by a saturable metabolic process (1). Other investigators have presented similar findings for monkeys and man (2–4). In addition, co-administration of dThd and FUra has been shown to result in a competitive metabolic interaction resulting in a prolonged half-life for FUra and increased clinical toxicity (5, 6).

For many compounds, plasma concentration vs. time data can be analyzed using one of a number of non-linear regression programs. In conjunction with an appropriate pharmacokinetic model, this procedure can provide valid estimates of the elimination rate constants and zero-time intercepts (7). However, when a compound is eliminated from the body by a saturable process the analysis becomes more complex, and simple first-order kinetics are no longer valid over a wide concentration range. Differential equations of the form:

$$\frac{-dC}{dt} = \frac{V_{max} \cdot C}{K_m + C} \quad (\text{Eq. 1})$$

where $-dC/dt$ is the rate of decline of drug concentration at time t , V_{max} is the maximum velocity (in concentration units) of the saturable process and K_m is the Michaelis constant, can be derived to describe such systems. Unfortunately, Equation 1 cannot be integrated and solved explicitly for C (7). It is difficult to use many non-linear regression programs to analyze this type of data, since they require an explicit expression for C . Some programs can accommodate a system of differential equations directly, but these can be costly of computational time (8), and in any case, a large number of unknown parameters may make a good fit difficult to obtain.

We have obtained estimates of V_{max} and K_m for dThd, Thy and FUra by incorporating these parameters into a series of balance equations describing the steady-state input and elimination of drug from the body during constant *i.v.* infusion (1).

¹ Department of Pharmacology, The George Washington University Medical Center, Washington, D. C. 20037

² From a dissertation presented to the Department of Pharmacology, The Graduate School of Arts and Sciences, The George Washington University, in partial fulfillment of the requirements for the degree of Doctor of Philosophy.

³ Present Address: Developmental Therapeutics Program, Division of Cancer Treatment, National Cancer Institute, NIH, Building 37, Room 5A15, Bethesda, MD 20205

⁴ To whom all correspondence and requests for reprints should be addressed.

⁵ This work was supported by National Cancer Institute Grants CA-22866 and T32-CA-09223.